

---

# SVDinsTN: An Integrated Method for Tensor Network Representation with Efficient Structure Search

---

Yu-Bang Zheng<sup>1</sup>, Xi-Le Zhao<sup>2,\*</sup>, Junhua Zeng<sup>3,4</sup>, Chao Li<sup>4</sup>, Qibin Zhao<sup>4</sup>,  
Heng-Chao Li<sup>1</sup>, Ting-Zhu Huang<sup>2</sup>

<sup>1</sup>School of Information Science and Technology, Southwest Jiaotong University

<sup>2</sup>School of Mathematical Sciences, University of Electronic Science and Technology of China

<sup>3</sup>School of Automation, Guangdong University of Technology

<sup>4</sup>Tensor Learning Team, RIKEN Center for Advanced Intelligence Project

\*Corresponding author

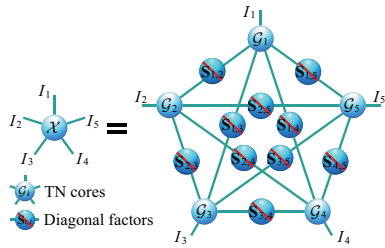
## Abstract

Tensor network (TN) representation is a powerful technique for data analysis and machine learning. It practically involves a challenging TN structure search (*TN-SS*) problem, which aims to search for the optimal structure to achieve a compact representation. Existing TN-SS methods mainly adopt a *bi-level* optimization method that leads to excessive computational costs due to repeated structure evaluations. To address this issue, we propose an efficient integrated (*single-level*) method named SVD-inspired TN decomposition (SVDinsTN), eliminating the need for repeated tedious structure evaluation. By inserting a diagonal factor for each edge of the fully-connected TN, we calculate TN cores and diagonal factors simultaneously, with *factor sparsity* revealing the most compact TN structure. Experimental results on real-world data demonstrate that SVDinsTN achieves approximately  $10 \sim 10^3$  times acceleration in runtime compared to the existing TN-SS methods while maintaining a comparable level of representation ability.

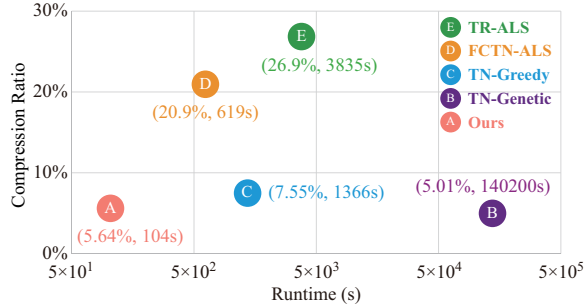
## 1 Introduction

Tensor network (TN) representation, which expresses higher-order data by low-dimensional tensors (called TN cores) with a specific operation among them, has gained significant attention in various areas of data analysis, machine learning, computer vision, etc [1, 3, 4, 10, 14, 24, 25, 26, 38]. By regarding TN cores as nodes and operations as edges, a TN corresponds to a graph (called TN topology) [8, 27, 33]. The vector composed of the weights of all edges in the topology is defined as the TN rank [33]. The selection of TN structure (including topology and rank) dramatically impacts the performance of TN representation in practical applications [13, 18, 22, 23, 30, 42]. Searching for a suitable TN structure to achieve a compact representation for a given tensor is called *TN structure search (TN-SS)*, which is known as a challenging and theoretically NP-hard problem [15, 18].

Recently, there have been several notable efforts to tackle the TN-SS problem [13, 18, 22, 30]. Most of these methods adopt a *bi-level* optimization framework, which is known to be computationally consuming [12, 31]. Specifically, these methods require sampling a large number of structures as candidates and conducting numerous repeated structure evaluations. For instance, TN-Genetic proposed in [18] requires thousands of structure evaluations for a tensor of size  $40 \times 60 \times 3 \times 9 \times 9$ . Consequently, the computational cost becomes exceedingly high, since each structure evaluation entails solving an optimization problem to iteratively compute TN cores from scratch. Designing a *single-level* optimization method as an alternative for the bi-level framework is expected to eliminate the repeated evaluations, thereby resulting in an efficient method for TN-SS.



(a) SVD-inspired TN decomposition



(b) Performance comparison of different methods

Figure 1: (a) A graphical representation of the proposed SVD-inspired TN decomposition on a fifth-order tensor. (b) Comparison of the compression ratio ( $\downarrow$ ) and runtime ( $\downarrow$ ) of different methods on a fifth-order light field image *Knights*, where the reconstruction error is set to 0.05, TR-ALS [40] and FCTN-ALS [42] are methods with pre-defined topologies, and TN-Greedy [13] and TN-Genetic [18] are TN-SS methods (Please see more results in Table 2).

In this paper, our goal is to construct an integrated (single-level) method for efficiently solving the TN-SS problem. To achieve this, we propose a novel method called *SVD-inspired TN decomposition* (*SVDinsTN*) that inserts diagonal factors between any two TN cores in the “fully-connected” topology (see Figure 1 (a) for illustration). The intuition behind *SVDinsTN* is to leverage the sparsity of the inserted diagonal factors to reveal the TN structure and utilize the TN cores (merged with diagonal factors) to represent the given tensor. Attributed to the single-level formulation, the TN cores and diagonal factors in *SVDinsTN* are updated simultaneously, and a sparse operator is imposed to induce the sparsity of the diagonal factors. Theoretically, we establish an upper bound for the TN rank involved in *SVDinsTN*, which serves as a guide for developing a novel initialization scheme for the diagonal factors and TN rank. This scheme allows *SVDinsTN* to overcome the high computational cost in the first several iterations. As a result, *SVDinsTN* is capable of capturing a customized TN structure and providing a compact representation for a given tensor in an efficient manner.

In summary, this paper makes the following two contributions:

- We propose *SVDinsTN* — a novel and highly efficient integrated method for TN representation with structure search.
- We surprisingly find from experimental results that the proposed method achieves approximately  $10 \sim 10^3$  times acceleration over state-of-the-art TN-SS methods with a comparable representation ability (Please see Figure 1 (b) for illustration).

## 1.1 Related works

**TN representation**<sup>1</sup> aims to find a set of small-sized TN cores to express a large-sized tensor under a TN structure (including topology and rank) [4, 5, 33]. In the past decades, many works focused on TN representation with a fixed TN topology, such as “chain” topology (tensor train (TT) decomposition [28, 37]), “ring” topology (tensor ring (TR) decomposition [35, 40]), “fully-connected” topology (fully-connected tensor network (FCTN) decomposition [42]), etc. In addition, these works also presented various methods to optimize the TN cores, such as alternating least square (ALS) [40], gradient descent (GD) [35, 37], proximal alternating minimization (PAM) [42], etc. Unlike these works, *SVDinsTN* in this paper is capable of handling TN-SS, a parasitically important problem arising from the fact that a pre-defined topology with a fixed rank would be not suitable (at least not optimal) for all possible tasks [18, 20, 29, 30, 34, 36, 39].

**TN structure search (TN-SS)** aims to search for a suitable or optimal TN structure, including both topology and rank, to achieve a compact representation for a given tensor [9, 13, 18, 19, 20, 22, 23, 25, 30]. However, most of these methods solve a bi-level optimization problem, such as greedy algorithm [13, 30] and genetic algorithm [18]. Consequently, these methods suffer from prohibitively

<sup>1</sup>Here we primarily focus on TN representation in scientific computing and machine learning, while acknowledging its long history of research in physics [6, 8, 16, 27, 33].

high computational costs due to the need for numerous repeated evaluations (each evaluation entails solving an optimization problem regarding the iterative calculation of TN cores). In contrast, the proposed SVDinsTN offers an integrated (single-level) method, in which we avoid the requirement for repeated structure evaluations, significantly decreasing the computational cost.

## 2 Notations and preliminaries

In this section, we first summarize notations and several operations that will be used in the rest of the paper. Then, we review definitions related to tensor networks (TNs).

A *tensor* is a multi-dimensional array, and the number of dimensions (also called *modes*) of which is referred to as the *tensor order*. In the paper, first-order tensors (vectors), second-order tensors (matrices), and  $N$ th-order tensors are denoted by  $\mathbf{x} \in \mathbb{R}^{I_1}$ ,  $\mathbf{X} \in \mathbb{R}^{I_1 \times I_2}$ , and  $\mathcal{X} \in \mathbb{R}^{I_1 \times I_2 \times \dots \times I_N}$ , respectively. We use  $\|\mathcal{X}\|_F$  and  $\|\mathcal{X}\|_1$  to denote the Frobenius norm and  $\ell_1$ -norm of  $\mathcal{X}$ , respectively. For brevity, we let  $\mathbb{K}_N$  denote the set  $\{1, 2, \dots, N\}$ , which is used for labeling individual indices. Similarly, we let  $\mathbb{T}\mathbb{L}_N$  denote the set  $\{(t, l) | 1 \leq t < l \leq N; t, l \in \mathbb{N}\}$ , which is used for labeling paired indices.

We next provide a review of several operations on tensors [42]. The *generalized tensor unfolding* is an operation that converts a tensor into a matrix by merging a group of tensor modes into the rows of the matrix and merging the remaining modes into the columns. For example, an  $I_1 \times I_2 \times I_3 \times I_4$  tensor can be unfolded into an  $I_1 I_3 \times I_2 I_4$  matrix, denoted by  $\mathbf{X}_{[1,3;2,4]}$ . We also use  $\mathbf{X}_{(2)}$  to simply represent  $\mathbf{X}_{[2;1,3,4]} \in \mathbb{R}^{I_2 \times I_1 I_3 I_4}$ , and use  $\mathcal{X} = \text{Fold}(\mathbf{X}_{(2)}, 2)$  to denote its corresponding inverse operation [17]. The *generalized tensor transposition* is an operation that rearranges tensor modes. For example, an  $I_1 \times I_2 \times I_3 \times I_4$  tensor can be transposed into an  $I_3 \times I_2 \times I_1 \times I_4$  tensor, denoted by  $\mathcal{X}^{\mathbf{n}}$  with  $\mathbf{n} = (3, 2, 1, 4)$ . The *tensor contraction* is an operation that obtains a new tensor by pairing, multiplying, and summing indices of certain modes of two tensors. For example, if a fourth-order tensor  $\mathcal{X} \in \mathbb{R}^{I_1 \times I_2 \times I_3 \times I_4}$  and a third-order tensor  $\mathcal{Y} \in \mathbb{R}^{J_1 \times J_2 \times J_3}$  satisfy  $I_2 = J_1$  and  $I_4 = J_2$ , then the tensor contraction between the 2nd and 4th modes of  $\mathcal{X}$  and the 1st and 2nd modes of  $\mathcal{Y}$  yields a tensor  $\mathcal{Z} = \mathcal{X} \times_{2,4}^{1,2} \mathcal{Y} \in \mathbb{R}^{I_1 \times I_3 \times J_3}$ . The elements of  $\mathcal{Z}$  are calculated as follows:

$$\mathcal{Z}(i_1, i_3, j_3) = \sum_{i_2=1}^{I_2} \sum_{i_4=1}^{I_4} \mathcal{X}(i_1, i_2, i_3, i_4) \mathcal{Y}(i_2, i_4, j_3).$$

We also use “abs”, “diag”, “mean”, “ones”, “reshape”, “size”, and “vec” to denote operations whose definitions are consistent with the corresponding Matlab commands.

### 2.1 Tensor network

In general, a *tensor network (TN)* is defined as a collection of low-dimensional tensors, known as TN cores, in which some or all modes are contracted according to specific operations [4, 5, 18, 33]. The primary purpose of a TN is to represent higher-order data using these TN cores. By considering TN cores as nodes and operations between modes of cores as edges, we define the graph formed by these nodes and edges as the TN topology. Additionally, we assign a non-negative integer weight to each edge to indicate the size of the corresponding TN core, and call the vector composed of these edge weights the TN rank. Consequently, a TN structure refers to a weighted graph comprising nodes, edges, and weights, encompassing both the TN topology and TN rank.

This paper focuses on a class of TNs that employs tensor contraction as the operation and adopts a simple graph as the topology. In particular, when representing an  $N$ th-order tensor  $\mathcal{X}$ , this class of TNs comprises precisely  $N$  TN cores, each corresponding to one mode of  $\mathcal{X}$ . A notable decomposition in this class is fully-connected tensor network (FCTN) decomposition [42]. FCTN decomposition represents an  $N$ th-order tensor  $\mathcal{X} \in \mathbb{R}^{I_1 \times I_2 \times \dots \times I_N}$  using  $N$  small-sized  $N$ th-order cores denoted by  $\mathcal{G}_k \in \mathbb{R}^{R_{1,k} \times R_{2,k} \times \dots \times R_{k-1,k} \times I_k \times R_{k,k+1} \times \dots \times R_{k,N}}$  for  $k \in \mathbb{K}_N$ . In this decomposition, any two cores  $\mathcal{G}_l$  and  $\mathcal{G}_t$  for  $(t, l) \in \mathbb{T}\mathbb{L}_N$  share an equal-sized mode  $R_{t,l}$  used for tensor contraction. We denote the FCTN decomposition by  $\mathcal{X} = \text{FCTN}(\mathcal{G}_1, \mathcal{G}_2, \dots, \mathcal{G}_N)$  and define the FCTN rank as the vector  $(R_{1,2}, R_{1,3}, \dots, R_{1,N}, R_{2,3}, \dots, R_{2,N}, \dots, R_{N-1,N}) \in \mathbb{R}^{N(N-1)/2}$ . According to the concept of tensor contraction, removing rank-one edges (with weight 1) in the TN topology does not change the expression of the TN. This means that if any element in the FCTN rank is equal to one, the corresponding edge can be harmlessly eliminated from the “fully-connected” topology. For

instance, a “fully-connected” topology with the rank  $(R_{1,2}, 1, \dots, 1, R_{2,3}, 1, \dots, 1, R_{N-1,N})$  can be converted into a “chain” topology with rank  $(R_{1,2}, R_{2,3}, \dots, R_{N-1,N})$  in this manner. This fact can be formally stated as follows.

**Property 1** [18, 21, 33] There exists a one-to-one correspondence between the *TN structure* and the *FCTN rank*.

In this work, we are inspired by Property 1, searching for more compact TN structures starting from the “fully-connected” topology.

### 3 SVDinsTN: an efficient integrated method for TN-SS

In this section, the new TN-SS method called SVDinsTN is introduced. Unlike the existing bi-level framework, the *main idea* of SVDinsTN is to insert a diagonal factor into each edge of the “fully-connected” topology, then to update TN cores and diagonal factors at the same level. The additional sparsity regularization for the inserted diagonal factors guides the method to reveal the most compact TN structure.

#### 3.1 SVD-inspired TN decomposition (SVDinsTN)

We start with the mathematical definition of SVDinsTN as follows.

**Definition 1 (SVDinsTN)** Let  $\mathcal{X} \in \mathbb{R}^{I_1 \times I_2 \times \dots \times I_N}$  be an *Nth-order tensor* such that

$$\begin{aligned} \mathcal{X}(i_1, i_2, \dots, i_N) = & \sum_{r_{1,2}=1}^{R_{1,2}} \sum_{r_{1,3}=1}^{R_{1,3}} \dots \sum_{r_{1,N}=1}^{R_{1,N}} \sum_{r_{2,3}=1}^{R_{2,3}} \dots \sum_{r_{2,N}=1}^{R_{2,N}} \dots \sum_{r_{N-1,N}=1}^{R_{N-1,N}} \\ & \mathbf{S}_{1,2}(r_{1,2}, r_{1,2}) \mathbf{S}_{1,3}(r_{1,3}, r_{1,3}) \dots \mathbf{S}_{1,N}(r_{1,N}, r_{1,N}) \\ & \mathbf{S}_{2,3}(r_{2,3}, r_{2,3}) \dots \mathbf{S}_{2,N}(r_{2,N}, r_{2,N}) \dots \\ & \mathbf{S}_{N-1,N}(r_{N-1,N}, r_{N-1,N}) \\ & \mathcal{G}_1(i_1, r_{1,2}, r_{1,3}, \dots, r_{1,N}) \\ & \mathcal{G}_2(r_{1,2}, i_2, r_{2,3}, \dots, r_{2,N}) \dots \\ & \mathcal{G}_k(r_{1,k}, r_{2,k}, \dots, r_{k-1,k}, i_k, r_{k,k+1}, \dots, r_{k,N}) \dots \\ & \mathcal{G}_N(r_{1,N}, r_{2,N}, \dots, r_{N-1,N}, i_N), \end{aligned} \quad (1)$$

where  $\mathcal{G}_k \in \mathbb{R}^{R_{1,k} \times R_{2,k} \times \dots \times R_{k-1,k} \times I_k \times R_{k,k+1} \times \dots \times R_{k,N}}$  for  $\forall k \in \mathbb{K}_N$  are *Nth-order tensors* and called *TN cores*, and  $\mathbf{S}_{t,l} \in \mathbb{R}^{R_{t,l} \times R_{t,l}}$  for  $\forall (t, l) \in \mathbb{TL}_N$  are *diagonal matrices*. Then we call (1) a *SVD-inspired TN decomposition (SVDinsTN)* of  $\mathcal{X}$ , denoted by  $\mathcal{X} = \text{STN}(\mathcal{G}, \mathbf{S})$ , where  $\mathcal{G}$  denotes  $\{\mathcal{G}_k | k \in \mathbb{K}_N\}$  and  $\mathbf{S}$  denotes  $\{\mathbf{S}_{t,l} | (t, l) \in \mathbb{TL}_N\}$ .

The proposed SVDinsTN draws inspiration from the well-known singular value decomposition (SVD) in linear algebra, but it is tailored to work with TN decomposition. We remark below the relationship between SVDinTN and matrix SVD, as well as the relationship with FCTN decomposition.

**SVDinTN and matrix SVD.** SVDinTN is essentially matrix SVD when TN cores satisfy an orthogonal constraint in the case of second-order tensors (matrices). This is because matrix SVD can be interpreted as inserting a diagonal matrix into these two smaller matrices obtained through matrix decomposition, where the number of non-zero elements in the diagonal matrix represents the matrix rank. When it comes to higher-order tensors, SVDinTN serves as a direct extension of matrix SVD, inheriting its fundamental ideas, and applying them to TN decomposition<sup>2</sup>.

**SVDinTN and FCTN decomposition.** SVDinsTN is a novel method that builds upon FCTN decomposition and enables the identification of the FCTN rank. It achieves this by inserting diagonal factors between any two TN cores in FCTN decomposition. The vector composed of the number of non-zero elements in these diagonal matrices is used to determine the FCTN rank. It is worth noting that SVDinTN can be transformed into an FCTN decomposition by merging the inserted diagonal factors into TN cores through the tensor contraction operation.

<sup>2</sup>We recognize that SVDinTN lacks theoretical properties of matrix SVD, which primary bottleneck lies in the difficulty of defining orthogonal forms of high-order tensors.

### 3.2 A single-level optimization method to calculate SVDinsTN

We now present the single-level optimization method for SVDinsTN (involving both the model and algorithm) that is capable of updating TN cores and diagonal factors simultaneously. In the method, we consider a weighted  $\ell_1$ -norm-based operator for  $\mathbf{S}$  and Tikhonov regularization [11] for  $\mathcal{G}$ . The  $\ell_1$ -norm-based operator is used to promote the sparsity of  $\mathbf{S}$ , and the Tikhonov regularization is used to restrict the feasible range of  $\mathcal{G}$ . To be specific, the proposed model is formulated as follows:

$$\min_{\mathcal{G}, \mathbf{S}} \frac{1}{2} \|\mathcal{X} - \text{STN}(\mathcal{G}, \mathbf{S})\|_F^2 + \sum_{\substack{1 \leq t < l \leq N \\ t, l \in \mathbb{N}}} \lambda_{t,l} \|\mathbf{S}_{t,l}\|_{\mathbf{w}_{t,l,1}} + \frac{\mu}{2} \sum_{k=1}^N \|\mathcal{G}_k\|_F^2, \quad (2)$$

where  $\lambda_{t,l} > 0$  for  $\forall (t, l) \in \mathbb{T}\mathbb{L}_N$  and  $\mu > 0$  are regularization parameters, and  $\|\mathbf{S}_{t,l}\|_{\mathbf{w}_{t,l,1}} := \|\mathbf{S}_{t,l} \odot \mathbf{W}_{t,l}\|_1$ . Here  $\mathbf{W}_{t,l} \in \mathbb{R}^{R_{t,l} \times R_{t,l}}$  for  $\forall (t, l) \in \mathbb{T}\mathbb{L}_N$  denote weight matrices that can be automatically updated according to  $\mathbf{S}_{t,l}$  and  $\odot$  denotes element-wise multiplication.

We use the PAM framework [2] to solve (2), whose solution is obtained by alternately updating

$$\begin{cases} \mathcal{G}_k = \underset{\mathcal{G}_k}{\text{argmin}} \frac{1}{2} \|\mathcal{X} - \text{STN}(\mathcal{G}, \mathbf{S})\|_F^2 + \frac{\mu}{2} \|\mathcal{G}_k\|_F^2 + \frac{\rho}{2} \|\mathcal{G}_k - \hat{\mathcal{G}}_k\|_F^2, \quad \forall k \in \mathbb{K}_N, \\ \mathbf{S}_{t,l} = \underset{\mathbf{S}_{t,l}}{\text{argmin}} \frac{1}{2} \|\mathcal{X} - \text{STN}(\mathcal{G}, \mathbf{S})\|_F^2 + \lambda_{t,l} \|\mathbf{S}_{t,l}\|_{\mathbf{w}_{t,l,1}} + \frac{\rho}{2} \|\mathbf{S}_{t,l} - \hat{\mathbf{S}}_{t,l}\|_F^2, \quad \forall (t, l) \in \mathbb{T}\mathbb{L}_N, \end{cases} \quad (3)$$

where  $\rho > 0$  is a proximal parameter (in this paper, we fix  $\rho = 0.001$ ), and  $\hat{\mathcal{G}}_k$  and  $\hat{\mathbf{S}}_{t,l}$  are the solutions of the  $\mathcal{G}_k$ -subproblem and  $\mathbf{S}_{t,l}$ -subproblem and at the previous iteration, respectively. By solving each sub-problem in (3), the updating rules of  $\mathcal{G}$  and  $\mathbf{S}$  are given as follows.

1) *Update  $\mathcal{G}_k$  for  $\forall k \in \mathbb{K}_N$ :* Solving the  $\mathcal{G}_k$ -subproblem requires fixing the other TN cores and diagonal factors. To address this, we use  $\mathbf{M}_k$  to denote the matrix obtained by performing tensor contraction and unfolding operations on all diagonal factors and TN cores except  $\mathcal{G}_k$ . Then, the  $\mathcal{G}_k$ -subproblem can be directly solved as follows:

$$\mathbf{G}_{k(k)} = (\mathbf{X}_{(k)} \mathbf{M}_k^T + \rho \hat{\mathbf{G}}_{k(k)}) (\mathbf{M}_k \mathbf{M}_k^T + (\mu + \rho) \mathbf{I})^{-1}. \quad (4)$$

2) *Update  $\mathbf{S}_{t,l}$  for  $\forall (t, l) \in \mathbb{T}\mathbb{L}_N$ :* Solving  $\mathbf{S}_{t,l}$ -subproblem requires fixing the other diagonal factors and TN cores. In a similar fashion, we use  $\mathbf{H}_{t,l}$  to denote the matrix obtained by performing tensor contraction and unfolding operations on all TN cores and diagonal factors except  $\mathbf{S}_{t,l}$ . Then, we use an alternating direction method of multipliers (ADMM) [7] to the  $\mathbf{S}_{t,l}$ -subproblem, which can be rewritten as follows:

$$\begin{aligned} \underset{\mathbf{s}_{t,l}}{\text{argmin}} \quad & \frac{1}{2} \|\mathbf{x} - \mathbf{H}_{t,l} \mathbf{q}_{t,l}\|_F^2 + \lambda_{t,l} \|\mathbf{s}_{t,l}\|_{\mathbf{w}_{t,l,1}} + \frac{\rho}{2} \|\mathbf{s}_{t,l} - \hat{\mathbf{s}}_{t,l}\|_F^2 \\ \text{s.t.} \quad & \mathbf{s}_{t,l} - \mathbf{q}_{t,l} = 0, \end{aligned} \quad (5)$$

where  $\mathbf{x} = \text{vec}(\mathcal{X})$ ,  $\mathbf{s}_{t,l} = \text{diag}(\mathbf{S}_{t,l})$ , and  $\mathbf{w}_{t,l} = \text{diag}(\mathbf{W}_{t,l})$ . The augmented Lagrangian function of (5) can be expressed as the following concise form:

$$\begin{aligned} L_{\beta_{t,l}}(\mathbf{s}_{t,l}, \mathbf{q}_{t,l}, \mathbf{p}_{t,l}) = & \frac{1}{2} \|\mathbf{x} - \mathbf{H}_{t,l} \mathbf{q}_{t,l}\|_F^2 + \lambda_{t,l} \|\mathbf{s}_{t,l}\|_{\mathbf{w}_{t,l,1}} \\ & + \frac{\rho}{2} \|\mathbf{s}_{t,l} - \hat{\mathbf{s}}_{t,l}\|_F^2 + \frac{\beta_{t,l}}{2} \left\| \mathbf{s}_{t,l} - \mathbf{q}_{t,l} + \frac{\mathbf{p}_{t,l}}{\beta_{t,l}} \right\|_F^2, \end{aligned} \quad (6)$$

where  $\mathbf{p}_{t,l}$  is the Lagrangian multiplier and  $\beta_{t,l}$  is the penalty parameter. Within the ADMM framework,  $\mathbf{s}_{t,l}$ ,  $\mathbf{q}_{t,l}$ , and  $\mathbf{p}_{t,l}$  can be solved by alternately updating

$$\begin{cases} \mathbf{q}_{t,l} = [\mathbf{H}_{t,l}^T \mathbf{H}_{t,l} + \beta_{t,l} \mathbf{I}]^{-1} [\mathbf{H}_{t,l}^T \mathbf{x} + \beta_{t,l} \mathbf{s}_{t,l} + \mathbf{p}_{t,l}], \\ \mathbf{s}_{t,l} = \text{shrink} \left( \frac{\rho \hat{\mathbf{s}}_{t,l} + \beta_{t,l} \mathbf{q}_{t,l} - \mathbf{p}_{t,l}}{\rho + \beta_{t,l}}, \frac{\lambda_{t,l} \mathbf{w}_{t,l}}{\rho + \beta_{t,l}} \right) \text{ with } \mathbf{w}_{t,l} = \frac{1}{\text{abs} \left( \frac{\rho \hat{\mathbf{s}}_{t,l} + \beta_{t,l} \mathbf{q}_{t,l} - \mathbf{p}_{t,l}}{\rho + \beta_{t,l}} \right) + \varepsilon}, \\ \mathbf{p}_{t,l} = \mathbf{p}_{t,l} + \beta_{t,l} (\mathbf{s}_{t,l} - \mathbf{q}_{t,l}), \end{cases} \quad (7)$$

where  $\varepsilon$  is a constant and  $\text{shrink}(\mathbf{a}, \mathbf{b}) = \max(\mathbf{a} - \mathbf{b}, \mathbf{0}) + \min(\mathbf{a} + \mathbf{b}, \mathbf{0})$ .

---

**Algorithm 1** An algorithm for calculate SVDinsTN.

---

**Input:** A tensor  $\mathcal{X} \in \mathbb{R}^{I_1 \times I_2 \times \dots \times I_N}$  and a parameter  $\gamma$ .

**Initialization:** Initialize  $\mathbf{S}_{t,l}$  and  $R_{t,l}$  by their initialization scheme and let  $\beta_{t,l} = 1$  for  $\forall(t,l) \in \mathbb{T}\mathbb{L}_N$ ; let  $\mathcal{G}_k = 1/\sqrt{I_k} \mathbf{ones}(R_{1,k}, R_{2,k}, \dots, R_{k-1,k}, I_k, R_{k,k+1}, \dots, R_{k,N})$  for  $\forall k \in \mathbb{K}_N$  and  $\mu = 1$ .

```
1: while not converged do
2:   Let  $\tilde{\mathcal{X}} = \mathcal{X}$  and  $\lambda_{t,l} = \gamma \max(\mathbf{S}_{t,l})(\rho + \beta_{t,l})$ .
3:   Update  $\mathcal{G}_k$  by (4) and let  $\mathcal{G}_k = \text{Fold}(\mathbf{G}_{k(k)}, k)$ .
4:   for  $i = 1$  to 5 do
5:     Update  $\mathbf{q}_{t,l}$ ,  $\mathbf{s}_{t,l}$ , and  $\mathbf{p}_{t,l}$  by (7).
6:   end for
7:   Delete the zero elements in  $\mathbf{s}_{t,l}$ , and let  $\mathbf{S}_{t,l} = \text{diag}(\mathbf{s}_{t,l})$  and  $R_{t,l} = \text{size}(\mathbf{s}_{t,l})$ .
8:   Delete the corresponding dimensions of  $\mathcal{G}_k$  and let  $\mathcal{X} = \text{STN}(\mathcal{G}, \mathbf{S})$ .
9:   Check the convergence condition:  $\|\mathcal{X} - \tilde{\mathcal{X}}\|_F / \|\tilde{\mathcal{X}}\|_F < 10^{-5}$ .
10: end while
```

**Output:**  $\mathcal{G}_k$  for  $\forall k \in \mathbb{K}_N$ , and  $\mathbf{S}_{t,l}$  and  $R_{t,l}$  for  $\forall(t,l) \in \mathbb{T}\mathbb{L}_N$ .

---

Taken together, we describe in Algorithm 1 the pseudocode to calculate SVDinsTN.

**Computational complexity.** For simplicity, we let the size of the  $N$ th-order tensor  $\mathcal{X}$  be  $I \times I \times \dots \times I$  and the initial FCTN rank be  $(R, R, \dots, R)$ . The computational cost involves updating  $\mathcal{G}$  and  $\mathbf{S}$ , resulting in a total cost of  $\mathcal{O}(N^3 I R^N + N \sum_{k=2}^N I^k R^{k(N-k)+k-1} + N I^{N-1} R^{2(N-1)} + N R^{3(N-1)})$  and  $\mathcal{O}(N^4 I R^N + N^2 R I^{2N} + N^2 R \sum_{k=2}^N I^k R^{k(N-k)+k-1})$ , respectively. In summary, the computational cost at each iteration is  $\mathcal{O}(N R^{3(N-1)} + N^4 I R^N + N^2 R I^{2N} + N^2 R \sum_{k=2}^N I^k R^{k(N-k)+k-1})$ .

### 3.3 Initialization scheme

SVDinsTN would encounter high computational cost in the first several iterations if the FCTN rank  $R_{t,l}$  for  $\forall(t,l) \in \mathbb{T}\mathbb{L}_N$  are initialized with large values. The issue is due to the utilization of a “fully-connected” topology as the starting point. To this end, we introduce a *novel* initialization scheme, which can effectively reduce the initial values of the FCTN rank  $R_{t,l}$  for  $\forall(t,l) \in \mathbb{T}\mathbb{L}_N$ . In this regard, we first give an upper bound for  $R_{t,l}$  in Theorem 1, by which we then propose a heuristic initialization scheme for both  $R_{t,l}$  and the diagonal factors  $\mathbf{S}_{t,l} \in \mathbb{R}^{R_{t,l} \times R_{t,l}}$  for  $\forall(t,l) \in \mathbb{T}\mathbb{L}_N$ .

**Theorem 1** Let  $\mathcal{X} \in \mathbb{R}^{I_1 \times I_2 \times \dots \times I_N}$  be an  $N$ th-order tensor, then there exists an SVD-inspired TN decomposition (1) with the FCTN rank  $R_{t,l} \leq \min(I_t, I_l)$  for  $\forall(t,l) \in \mathbb{T}\mathbb{L}_N$ .

Considering  $R_{t,l}$  is related to the correlation between the  $t$ th and  $l$ th modes of an  $N$ th-order tensor  $\mathcal{X} \in \mathbb{R}^{I_1 \times I_2 \times \dots \times I_N}$ , we initialize  $R_{t,l}$  and  $\mathbf{S}_{t,l}$  by virtue of matrix SVD of mode- $(t,l)$  slices<sup>3</sup> of  $\mathcal{X}$ . This initialization scheme consists of two steps:

*Step 1: Calculate  $\mathbf{X}_{t,l}$ , i.e., the mean of all mode- $(t,l)$  slices of  $\mathcal{X}$ . We first define*

$$\mathcal{X}_{t,l} = \text{reshape} \left( \vec{\mathcal{X}}^{\mathbf{n}}, I_t, I_l, \prod_{\substack{i=1 \\ i \neq t,l}}^N I_i \right) \text{ and then let } \mathbf{X}_{t,l} = \text{mean}(\mathcal{X}_{t,l}, 3) \in \mathbb{R}^{I_t \times I_l},$$

where  $\mathbf{n} = (t, l, 1, 2, \dots, t-1, t+1, \dots, l-1, l+1, \dots, N)$ .

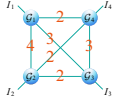
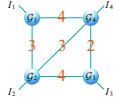
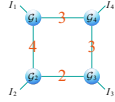
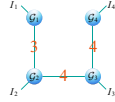
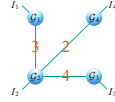
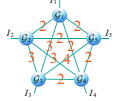
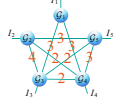
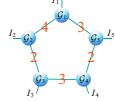
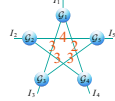
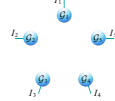
*Step 2: Calculate the initial  $R_{t,l}$  and  $\mathbf{S}_{t,l}$ .* First, we perform matrix SVD on  $\mathbf{X}_{t,l}$  to obtain  $\mathbf{s}_{t,l} \in \mathbb{R}^{\min(I_t, I_l)}$ , whose elements are singular values of  $\mathbf{X}_{t,l}$ . Then, we let  $\mathbf{s}_{t,l} = \text{shrink}(\mathbf{s}_{t,l}, \frac{\gamma \max(\mathbf{s}_{t,l})}{\text{abs}(\mathbf{s}_{t,l}) + \varepsilon})$  and delete zero elements in  $\mathbf{s}_{t,l}$ . Final, we let  $\mathbf{S}_{t,l} = \text{diag}(\mathbf{s}_{t,l})$  and  $R_{t,l} = \text{size}(\mathbf{s}_{t,l})$ .

In practical applications, the *shrink* operation in Step 2 effectively reduces the initial value of the  $R_{t,l}$  by projecting very small singular values in  $\mathbf{s}_{t,l}$  to zero. As a result, the challenge of high computational costs in the first several iterations of SVDinTN can be effectively addressed. The efficiency of the initialization scheme is numerically illustrated in Figure 2.

---

<sup>3</sup>Mode- $(t,l)$  slices are two-dimensional sections, obtained by fixing all but the mode- $t$  and the mode- $l$  indexes, of a tensor [41].

Table 1: Performance of SVDinsTN on TN structure revealing under 100 independent tests

True structure (4th-order)					
Success rate	100%	100%	96%	95%	99%
True structure (5th-order)					
Success rate	100%	98%	96%	97%	100%

## 4 Numerical experiments

In this section, we present numerical experiments conducted on both synthetic and real-world data to evaluate the performance of the proposed SVDinsTN method. The primary objective is to validate the following three Claims:

- A: SVDinsTN can reveal a customized TN structure that aligns with the unique structure of a given tensor.
- B: SVDinsTN can significantly reduce time costs while achieving comparable representation ability to state-of-the-art TN-SS methods. Moreover, SVDinsTN can surpass methods with pre-defined topologies regarding representation ability.
- C: SVDinsTN can outperform existing tensor decomposition methods in the tensor completion task, highlighting its effectiveness as a valuable tool in practical applications.

### 4.1 Experiments for validating Claim A

First of all, we conduct experiments to validate Claim A. Real-world data lacks a true TN structure, and thus we consider synthetic data in this experiment.

**Data generation.** We first randomly generate  $\mathcal{G}_k \in \mathbb{R}^{R_{1,k} \times R_{2,k} \times \dots \times R_{k-1,k} \times I_k \times R_{k,k+1} \times \dots \times R_{k,N}}$  for  $\forall k \in \mathbb{K}_N$  and  $\mathbf{S}_{t,l} \in \mathbb{R}^{R_{t,l} \times R_{t,l}}$  for  $\forall (t, l) \in \mathbb{TL}_N$ , whose elements are taken from a uniform distribution between 0 and 1. Then we obtain the synthetic tensor by  $\mathcal{X} = \text{STN}(\mathcal{G}, \mathbf{S})$ .

**Experiment setting.** We test both fourth-order tensors of size  $16 \times 18 \times 20 \times 22$  and fifth-order tensors of size  $14 \times 16 \times 18 \times 20 \times 22$ , and consider five different kinds of TN structures. For each structure, we conduct 100 independent tests and regenerate the synthetic data to ensure reliable and unbiased results. The ability of the proposed SVDinsTN to reveal TN structure is measured by the *success rate* of the output structures, defined as  $S_T/T \times 100\%$ , where  $T = 100$  is the total number of tests and  $S_T$  is the number of tests that accurately output the true TN structure. In all tests, the parameter  $\gamma$  is set to 0.0015.

**Result analysis.** Table 1 presents the *success rate* of the output TN structures obtained by the proposed SVDinsTN in 100 independent tests on fourth-order and fifth-order tensors. It can be observed that the proposed SVDinsTN consistently yields high *success rates* of over 95% in all test cases. Notably, in approximately half of the test cases, the *success rates* reach a perfect score of 100%. Moreover, it is also worth mentioning that in the test on fifth-order tensors, we consider two isomorphic topologies: the “ring” topology and the “five-star” topology. These two topologies are both the “ring” topology (TR decomposition), but with different permutations:  $\mathcal{G}_1 \rightarrow \mathcal{G}_2 \rightarrow \mathcal{G}_3 \rightarrow \mathcal{G}_4 \rightarrow \mathcal{G}_5 \rightarrow \mathcal{G}_1$  and  $\mathcal{G}_1 \rightarrow \mathcal{G}_3 \rightarrow \mathcal{G}_5 \rightarrow \mathcal{G}_2 \rightarrow \mathcal{G}_4 \rightarrow \mathcal{G}_1$ , respectively. It can be seen that despite the isomorphism, the proposed SVDinsTN can accurately identify the correct permutation for each topology.

### 4.2 Experiments for validating Claim B

In this subsection, we conduct experiments to validate Claim B. We consider real-world data and use different methods to represent it in this experiment.

Table 2: Comparison of the CR ( $\downarrow$ ) and runtime ( $\times 1000s$ ,  $\downarrow$ ) of different methods on light field data

Data	Method	RE bound: 0.01		RE bound: 0.05		RE bound: 0.1	
		CR	Runtime	CR	Runtime	CR	Runtime
 <i>Bunny</i>	TR-ALS [40]	60.5%	13.54	17.4%	0.471	5.31%	0.118
	FCTN-ALS [42]	65.1%	13.08	20.9%	0.473	3.93%	0.041
	TN-Greedy [13]	26.1%	11.02	6.32%	1.021	2.34%	0.362
	TN-Genetic [18]	27.9%	1014	<u>5.01%</u>	180.3	<u>2.25%</u>	12.52
	SVDinsTN	<u>22.4%</u>	<b>0.745</b>	6.92%	<b>0.029</b>	2.66%	<b>0.005</b>
 <i>Knights</i>	TR-ALS [40]	74.7%	10.31	26.9%	3.835	9.15%	0.423
	FCTN-ALS [42]	73.5%	12.35	20.9%	0.619	3.93%	<b>0.014</b>
	TN-Greedy [13]	32.1%	12.53	7.55%	1.366	3.50%	0.481
	TN-Genetic [18]	38.7%	912.9	<u>5.01%</u>	140.2	<u>2.44%</u>	12.52
	SVDinsTN	<u>32.0%</u>	<b>1.548</b>	5.64%	<b>0.104</b>	2.76%	0.019
 <i>Truck</i>	TR-ALS [40]	62.8%	17.62	22.6%	1.738	6.00%	0.090
	FCTN-ALS [42]	69.3%	7.735	20.9%	2.953	3.93%	0.159
	TN-Greedy [13]	26.9%	6.676	7.26%	1.259	3.35%	0.488
	TN-Genetic [18]	27.9%	1014	<u>5.01%</u>	170.3	2.85%	12.52
	SVDinsTN	<u>23.5%</u>	<b>1.051</b>	6.42%	<b>0.152</b>	<u>2.83%</u>	<b>0.023</b>

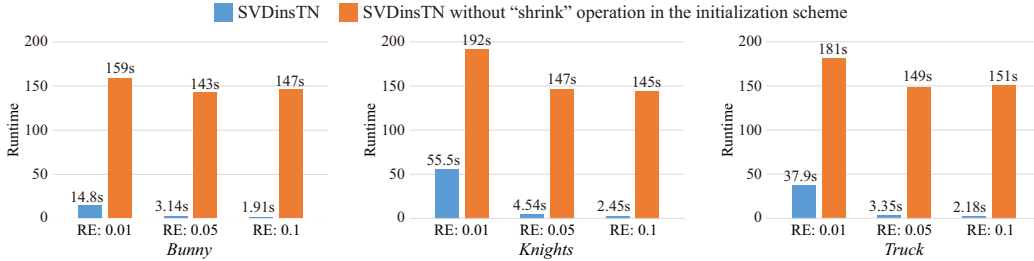


Figure 2: Runtime comparison of the first five iterations between SVDinsTN and SVDinsTN without the shrink operation in the initialization scheme.

**Experiment setting.** We test three light field data<sup>4</sup>, named *Bunny*, *Knights*, and *Truck*, all of which are fifth-order tensors of size  $40 \times 60 \times 3 \times 9 \times 9$  (spatial height  $\times$  spatial width  $\times$  color channel  $\times$  vertical grid  $\times$  horizontal grid). We employ four representative methods as the compared baselines, including two methods with pre-defined topology: TR-ALS [40] and FCTN-ALS [42], and two TN-SS methods: TN-Greedy [13] and TN-Genetic [18]. We represent the test light field data by different methods and calculate the corresponding *compression ratio* (*CR*) to achieve a certain *reconstruction error* (*RE*). The *CR* is defined as  $F_G/F_{\mathcal{X}} \times 100\%$ , where  $F_G$  is the number of elements of TN cores used to represent a tensor and  $F_{\mathcal{X}}$  is the number of total elements of the original tensor. The *RE* is defined as  $\|\mathcal{X} - \hat{\mathcal{X}}\|_F / \|\mathcal{X}\|_F$ , where  $\mathcal{X}$  is the original data and  $\hat{\mathcal{X}}$  is the reconstructed data. In all tests, we select the parameter  $\gamma$  from the interval  $[10^{-7}, 10^{-3}]$ .

**Result analysis.** Table 2 reports the *CR* and *runtime* of different methods on representing fifth-order light field data. The results show that the proposed SVDinsTN achieves significantly lower *CR* and *time costs* than TR-ALS and FCTN-ALS, which are methods with pre-defined topology. Compared to TN-Greedy and TN-Genetic, the proposed SVDinsTN achieves a speed improvement of approximately  $10 \sim 10^3$  times with a comparable level of *CR*. This is because TN-Greedy and TN-Genetic necessitate a significant number of repeated evaluations of the objective function, whereas our method only requires a single evaluation.

**Impact of the initialization scheme.** We also analyze the impact of the shrink operation in the initialization scheme under this experimental setting. Figure 2 presents the runtime comparison of the initial five iterations between SVDinsTN with the shrink operation and SVDinsTN without the shrink operation in the initialization scheme. The results demonstrate that the designed initialization

<sup>4</sup>The data is available at <http://lightfield.stanford.edu/lfs.html>.

Table 3: Comparison of MPSNR ( $\uparrow$ ) and runtime (s,  $\downarrow$ ) of different TC methods on color videos

Video	FBCP [39]		TMac [32]		TMacTT [32]		TRLRF [36]		SVDinsTN	
	MPSNR	Runtime	MPSNR	Runtime	MPSNR	Runtime	MPSNR	Runtime	MPSNR	Runtime
<i>Bunny</i>	28.402	1731	28.211	1203	29.523	453.7	29.163	486.7	<b>32.366</b>	482.8
<i>News</i>	28.234	1720	27.882	<u>340.4</u>	28.714	535.9	28.857	978.1	<b>31.574</b>	751.8
<i>Salesman</i>	29.077	1783	28.469	<u>353.6</u>	29.534	656.4	28.288	689.3	<b>31.671</b>	512.5
<i>Silent</i>	30.126	1453	30.599	316.2	30.647	1305	31.081	453.2	<b>32.012</b>	<u>208.1</u>

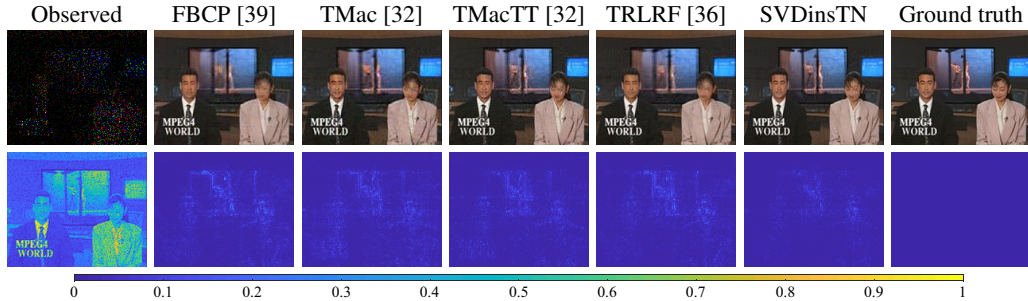


Figure 3: Reconstructed images and the corresponding residual images on the 25th frame of *News*.

scheme significantly reduces the computational costs in the first several iterations of SVDinTN. These findings validate the analysis presented in Section 3.3.

### 4.3 Experiments for validating Claim C

In this subsection, we conduct experiments to validate Claim C. We employ the proposed SVDinsTN to a fundamental application, i.e., tensor completion (TC), and compare it with the state-of-the-art tensor decomposition-based TC methods. Given an incomplete observation tensor  $\mathcal{F} \in \mathbb{R}^{I_1 \times I_2 \times \dots \times I_N}$  of  $\mathcal{X} \in \mathbb{R}^{I_1 \times I_2 \times \dots \times I_N}$ , the proposed TC method first updates  $\mathcal{G}$  and  $\mathbf{S}$  by Algorithm 1, and then update the target tensor  $\mathcal{X}$  as follows:  $\mathcal{X} = \mathcal{P}_{\Omega^c}((\text{STN}(\mathcal{G}, \mathbf{S}) + \rho \hat{\mathcal{X}})/(1 + \rho)) + \mathcal{P}_{\Omega}(\mathcal{F})$ , where  $\Omega$  is the index set of the known elements,  $\mathcal{P}_{\Omega}(\mathcal{X})$  is a projection operator which projects the elements in  $\Omega$  to themselves and all others to zeros,  $\hat{\mathcal{X}}$  is the result at the previous iteration, and the initial  $\hat{\mathcal{X}}$  is  $\mathcal{F}$ .

**Experiment setting.** We test four color video data<sup>5</sup>, named *Bunny*, *News*, *Salesman*, and *Silent*, all of which are fourth-order tensors of size  $144 \times 176 \times 3 \times 50$  (spatial height  $\times$  spatial width  $\times$  color channel  $\times$  frame). We employ four baseline methods for comparison, named FBCP [39], TMac [32], TMacTT [3], and TRLRF [36], respectively. These methods are based on different tensor decompositions. We set the missing ratio (MR) to 90%, where MR is the ratio of the number of missing elements to the total number of elements. We evaluate the reconstructed quality by *the mean peak signal-to-noise ratio (MPSNR)* computed across all frames. In all tests, the parameter  $\gamma$  is set to 0.0003.

**Result analysis.** Table 3 reports *MPSNR* and *runtime* obtained by different TC methods on test color videos. As observed, the proposed SVDinsTN consistently achieves the highest *MPSNR* values among all utilized TC methods across all test color videos. Besides, SVDinsTN exhibits comparable *runtime* to the baseline methods. Figure 3 displays the reconstructed images and their corresponding residual images at the 25th frame of *News*. We observe that the proposed SVDinsTN outperforms the baseline methods in terms of visual quality, particularly with respect to background cleanliness and local details (e.g. “dancer”) recovery.

## 5 Conclusion

**Summary.** We propose SVDinTN, an integrated method for tensor network representation with structure search. SVDinTN outperforms methods with pre-defined topologies in terms of repre-

<sup>5</sup>The data is available at <http://trace.eas.asu.edu/yuv/>.

sensation ability and achieves a significant speedup of approximately  $10 \sim 10^3$  times compared to state-of-the-art TN-SS methods while maintaining comparable representation ability. Additionally, SVDinTN demonstrates its effectiveness as a valuable tool in practical applications.

**Limitations.** Despite the substantial acceleration achieved by our method, there are instances where it exhibits a slightly higher compression ratio (CR) compared to the TN-Genetic baseline method. This discrepancy arises because TN-Genetic explores nearly all possible TN topologies in these experiments. Solving this issue will be the direction of our future work.

## Acknowledgments

We would like to express our gratitude to Guillaume Rabusseau for his valuable assistance in correcting the experimental results of “TN-Greedy”.

## References

- [1] A. Anandkumar, R. Ge, D. Hsu, S. M. Kakade, and M. Telgarsky. Tensor decompositions for learning latent variable models. *The Journal of Machine Learning Research*, 15(1):2773–2832, 2014.
- [2] H. Attouch, J. Bolte, P. Redont, and A. Soubeyran. Proximal alternating minimization and projection methods for nonconvex problems: An approach based on the Kurdyka-Łojasiewicz inequality. *Mathematics of Operations Research*, 35(2):438–457, 2010.
- [3] J. A. Bengua, H. N. Phien, H. D. Tuan, and M. N. Do. Efficient tensor completion for color image and video recovery: Low-rank tensor train. *IEEE Transactions on Image Processing*, 26(5):2466–2479, 2017.
- [4] A. Cichocki, N. Lee, I. Oseledets, A.-H. Phan, Q. Zhao, and D. P. Mandic. Tensor networks for dimensionality reduction and large-scale optimization: Part 1 low-rank tensor decompositions. *Foundations and Trends® in Machine Learning*, 9(4-5):249–429, 2016.
- [5] A. Cichocki, D. Mandic, L. De Lathauwer, G. Zhou, Q. Zhao, C. Caiafa, and H. A. PHAN. Tensor decompositions for signal processing applications: From two-way to multiway component analysis. *IEEE Signal Processing Magazine*, 32(2):145–163, 2015.
- [6] M. Fannes, B. Nachtergaele, and R. F. Werner. Finitely correlated states on quantum spin chains. *Communications in Mathematical Physics*, 144(3):443–490, 1992.
- [7] D. Gabay and B. Mercier. A dual algorithm for the solution of nonlinear variational problems via finite element approximation. *Computers and Mathematics with Applications*, 2(1):17–40, 1976.
- [8] S. Garnerone, T. R. de Oliveira, and P. Zanardi. Typicality in random matrix product states. *Physical Review A*, 81:032336, 2010.
- [9] M. Ghadiri, M. Fahrback, G. Fu, and V. Mirrokni. Approximately optimal core shapes for tensor decompositions. *arXiv preprint arXiv:2302.03886*, 2023.
- [10] I. Glasser, R. Sweke, N. Pancotti, J. Eisert, and J. I. Cirac. Expressive power of tensor-network factorizations for probabilistic modeling. In *Advances in Neural Information Processing Systems*, volume 32, 2019.
- [11] G. H. Golub, P. C. Hansen, and D. P. O’Leary. Tikhonov regularization and total least squares. *SIAM journal on matrix analysis and applications*, 21(1):185–194, 1999.
- [12] P. Hansen, B. Jaumard, and G. Savard. New branch-and-bound rules for linear bilevel programming. *SIAM Journal on Scientific and Statistical Computing*, 13(5):1194–1217, 1992.
- [13] M. Hashemizadeh, M. Liu, J. Miller, and G. Rabusseau. Adaptive learning of tensor network structures. *arXiv preprint arXiv:2008.05437*, 2020.
- [14] K. Hayashi, T. Yamaguchi, Y. Sugawara, and S.-i. Maeda. Exploring unexplored tensor network decompositions for convolutional neural networks. In *Advances in Neural Information Processing Systems*, volume 32, 2019.
- [15] C. J. Hillar and L.-H. Lim. Most tensor problems are NP-hard. *Journal of the ACM*, 60(6):1–39, 2013.
- [16] R. Hübener, V. Nebendahl, and W. Dür. Concatenated tensor network states. *New journal of physics*, 12(2):025004, 2010.
- [17] T. G. Kolda and B. W. Bader. Tensor decompositions and applications. *SIAM Review*, 51(3):455–500, 2009.
- [18] C. Li and Z. Sun. Evolutionary topology search for tensor network decomposition. In *Proceedings of the 37th International Conference on Machine Learning*, volume 119, pages 5947–5957, 2020.

- [19] C. Li, J. Zeng, C. Li, C. Caiafa, and Q. Zhao. Alternating local enumeration (tnale): Solving tensor network structure search with fewer evaluations. *arXiv preprint arXiv:2304.12875*, 2023.
- [20] C. Li, J. Zeng, Z. Tao, and Q. Zhao. Permutation search of tensor network structures via local sampling. In *Proceedings of the 39th International Conference on Machine Learning*, volume 162, pages 13106–13124, 2022.
- [21] C. Li and Q. Zhao. Is rank minimization of the essence to learn tensor network structure? In *Second Workshop on Quantum Tensor Networks in Machine Learning (QTNML)*, Neurips, 2021.
- [22] N. Li, Y. Pan, Y. Chen, Z. Ding, D. Zhao, and Z. Xu. Heuristic rank selection with progressively searching tensor ring network. *Complex & Intelligent Systems*, 8(2):771–785, 2022.
- [23] Y. Liu, Y. Lu, W. Ou, Z. Long, and C. Zhu. Adaptively topological tensor network for multi-view subspace clustering. *arXiv preprint arXiv:2305.00716*, 2023.
- [24] O. A. Malik, V. Bharadwaj, and R. Murray. Sampling-based decomposition algorithms for arbitrary tensor networks. *arXiv preprint arXiv:2210.03828*, 2022.
- [25] C. Nie, H. Wang, and L. Tian. Adaptive tensor networks decomposition. In *British Machine Vision Conference*, 2021.
- [26] M. Nimishakavi, P. K. Jawanpuria, and B. Mishra. A dual framework for low-rank tensor completion. In *Advances in Neural Information Processing Systems*, volume 31, 2018.
- [27] R. Orús. A practical introduction to tensor networks: Matrix product states and projected entangled pair states. *Annals of Physics*, 349:117–158, 2014.
- [28] I. V. Oseledets. Tensor-train decomposition. *SIAM Journal on Scientific Computing*, 33(5):2295–2317, 2011.
- [29] P. Rai, Y. Wang, S. Guo, G. Chen, D. Dunson, and L. Carin. Scalable bayesian low-rank decomposition of incomplete multiway tensors. In *Proceedings of the 31st International Conference on International Conference on Machine Learning*, volume 32, page II–1800–II–1808, 2014.
- [30] F. Sedighin, A. Cichocki, and A.-H. Phan. Adaptive rank selection for tensor ring decomposition. *IEEE Journal of Selected Topics in Signal Processing*, 15(3):454–463, 2021.
- [31] A. Sinha, P. Malo, and K. Deb. A review on bilevel optimization: From classical to evolutionary approaches and applications. *IEEE Transactions on Evolutionary Computation*, 22(2):276–295, 2018.
- [32] Y. Xu, R. Hao, W. Yin, and Z. Su. Parallel matrix factorization for low-rank tensor completion. *Inverse Problems and Imaging*, 9(2):601–624, 2015.
- [33] K. Ye and L.-H. Lim. Tensor network ranks. *arXiv preprint arXiv:1801.02662*, 2018.
- [34] T. Yokota, Q. Zhao, and A. Cichocki. Smooth parafac decomposition for tensor completion. *IEEE Transactions on Signal Processing*, 64(20):5423–5436, 2016.
- [35] L. Yuan, J. Cao, X. Zhao, Q. Wu, and Q. Zhao. Higher-dimension tensor completion via low-rank tensor ring decomposition. In *Asia-Pacific Signal and Information Processing Association Annual Summit and Conference*, pages 1071–1076, 2018.
- [36] L. Yuan, C. Li, D. Mandic, J. Cao, and Q. Zhao. Tensor ring decomposition with rank minimization on latent space: An efficient approach for tensor completion. In *Proceedings of the AAAI Conference on Artificial Intelligence*, volume 33, pages 9151–9158, 2019.
- [37] L. Yuan, Q. Zhao, L. Gui, and J. Cao. High-order tensor completion via gradient-based optimization under tensor train format. *Signal Processing: Image Communication*, 73:53–61, 2019.
- [38] Q. Zhao, C. F. Caiafa, D. Mandic, L. Zhang, T. Ball, A. Schulze-bonhage, and A. Cichocki. Multilinear subspace regression: An orthogonal tensor decomposition approach. In *Advances in Neural Information Processing Systems*, volume 24, 2011.
- [39] Q. Zhao, L. Zhang, and A. Cichocki. Bayesian CP factorization of incomplete tensors with automatic rank determination. *IEEE Transactions on Pattern Analysis and Machine Intelligence*, 37(9):1751–1763, 2015.
- [40] Q. Zhao, G. Zhou, S. Xie, L. Zhang, and A. Cichocki. Tensor ring decomposition. *arXiv preprint arXiv:1606.05535*, 2016.
- [41] Y.-B. Zheng, T.-Z. Huang, X.-L. Zhao, T.-X. Jiang, T.-Y. Ji, and T.-H. Ma. Tensor N-tubal rank and its convex relaxation for low-rank tensor recovery. *Information Sciences*, 532:170–189, 2020.
- [42] Y.-B. Zheng, T.-Z. Huang, X.-L. Zhao, Q. Zhao, and T.-X. Jiang. Fully-connected tensor network decomposition and its application to higher-order tensor completion. In *Proceedings of the AAAI Conference on Artificial Intelligence*, volume 35, pages 11071–11078, 2021.